GEOPHYSICS, VOL. 41, NO. 1 (FEBRUARY, 1976), P. 62–78, 12 FIGS.

FINITE-DIFFERENCE RESISTIVITY MODELING FOR ARBITRARILY SHAPED TWO-DIMENSIONAL STRUCTURES

IRSHAD R. MUFTI*

Resistivity surveying is commonly done by using a point-source dipole. Consequently, a finite-difference evaluation of apparent resistivity curves implies the use of three-dimensional simulation models which necessitate prohibitive computer costs. However, if we assume variation of resistivity only in two dimensions and use a line-source dipole for setting up the finite-difference model of a given structure, the potential field can be evaluated easily.

A discrete version of the resistivity problem in two dimensions, which takes into account nonuniform grid spacing, is presented as a system of self-adjoint difference equations. Since the iterative solution of such a system does not require grid spacing to be less than a certain critical value, it was successfully used for the development of fast-convergence finite-difference models. By examining in detail the characteristics of the matrix associated with the evaluation of the potential field, it is demonstrated that the proposed modeling procedure will remain stable for all conceivable geometries and resistivity distributions. It was used for the investigation of certain models for which the corresponding results could also be computed analytically. A direct superposition of results obtained in the two cases shows that they are virtually identical. By making use of the reciprocity theorem, a computational short-cut, which provides the evaluation of vertical sounding curves for a line-source dipole in a single step, is put forward.

Special problems related to the optimization of acceleration parameters as well as the estimation of the potential function along the subsurface boundaries of the model are discussed. It is concluded that by surrounding the model by a termination strip of very large effective width, either Neumann- or Dirichlet-type boundary conditions can be used for simulating a semiinfinite medium without introducing signficant errors in the results.

INTRODUCTION

The interpretation of electrical resistivity field data is commonly done by assuming that the subsurface consists of a system of uniform and homogeneous parallel layers. Very often this assumption amounts to a gross simplification of the actual geology. A much more realistic model of the subsurface can be constructed by making provision for the variation of resistivity in two directions. Very often, the error introduced by assuming no variation of resistivity along the third direction can be minimized by choosing the direction of the measurement profile at right angles to the direction of strike. In situations where such a choice is not possible, this error will not adversely affect the interpretation of field data because most of the current supplied to the ground is concentrated in the zone adjacent to the vertical cross-section containing the current electrodes.

If we further assume that the current is supplied to the ground by means of a pair of infinite line electrodes, extending at right angles to the direction of the measurement profile, the resistivity problem can be treated as purely two-dimensional and can be solved easily by a finite-difference scheme.

Paper presented at the 44th Annual International SEG Meeting, November 12, 1974 in Dallas, Tex. Manuscript received by the Editor February 18, 1975; revised manuscript received May 7, 1975.
* Amoco Production Co., Tulsa, Okla. 74102.

We shall base our treatment on this assumption of a line-source dipole and shall be concerned with the finite-difference evaluation of the potential field and apparent resistivity curves for two-dimensional structures of arbitrary shape. Studies of this problem along these lines were recently reported by Jepsen (1969) and Aiken et al (1973). Both have attempted solving this problem by using the straightforward relaxation method due to Southwell (1946), which is much too slow even on modern high-speed computers. Moreover, the finite-difference scheme presented in both cases becomes unstable except for certain resistivity ratios and specific subsurface geometries. In the following pages, fast-convergence finite-difference systems based on the stability analysis of the resistivity problem will be discussed in detail.

FUNDAMENTAL RELATIONS

The flow of steady electric current in a nonuniform medium containing a current source is governed by the relation

$$-\nabla \cdot \left[\frac{1}{\rho(x, y, z)} \nabla v(x, y, z)\right] = \frac{\partial Q(x, y, z)}{\partial t}, \qquad (1)$$

where ρ is the resistivity of the medium [ohm-m], v is the electric scalar potential [volt], Q is the charge density [coul m^{-3}]. We shall simplify the notations by substituting

$$\frac{\partial Q}{\partial t} = q(x, y, z)$$

and

$$1/\rho(x, y, z) = \sigma(x, y, z)$$

where q is the current density [amp m^{-3}] and σ is the conductivity of the medium [mhos m^{-1}].

When the system represented by (1) is restricted to two dimensions (x, z), we obtain

$$\frac{\partial}{\partial x}\left[\sigma(x, z)\frac{\partial v}{\partial x}\right] + \frac{\partial}{\partial z}\left[\sigma(x, z)\frac{\partial v}{\partial z}\right] + q(x, z) = 0. \qquad (2)$$

In (2), q must now be interpreted as a variable current density in amp/m^2 in a typical two-dimensional xz cross-section but per meter length in the third direction, y. Relation (2) represents an example of a self-adjoint elliptic system (Young, 1962). Such systems occur very frequently and can be accurately solved by a finite-difference relaxation technique.

In the resistivity method, both the source (positive current electrode) and the sink (negative current electrode) are located at the surface of the ground; however, the following treatment is more general and permits the location of current electrodes anywhere in the medium.

RESISTIVITY PROBLEM DISCRETIZED

For the purpose of finite-difference modeling, the semiinfinite medium must be made finite by introducing an artificial boundary. Such a boundary is seen in Figure 1, which represents a vertical cross-section of the ground. The portion of the boundary from A to B corresponds to the surface of the ground, whereas the remaining boundary of the model, $BCDA$, is fictitious. The continuous medium can not be discretized by dividing it into a number of rectangular cells and replacing each cell by a point. Thus, the point P represents the rectangular area $abcd$. We shall call each of these points an element of the discretized medium. In order to emphasize the fact that the corrdinates (x, z) of an element can only take on integral values, the coordinates will be expressed as (i, j). Moreover, to simplify the treatment to follow, the origin $(x = 0, z = 0)$ will correspond to $(i = 1, j = 0)$.

Since the current supplied to the ground by means of electrodes is commonly expressed in amperes, whereas the current density q appearing in (2) represents the rate of charge generation (or absorption) per unit area, it would be desirable to express q in terms of the current flowing into the ground. Suppose the element P (Figure 1) represents the location of a current electrode supplying I amperes into the subsurface. Let us denote its neighboring elements by E, W, N, and S (Figure 2). Since the point P represents the shaded area $abcd$, the current density q_P due to the electrode at P will be given by

$$q_P = I/(\text{Area } abcd) = 4I/[(h_E + h_W)(h_N + h_S)]. \qquad (3)$$

Now we consider the case

$$\lim_{h_N \to 0} q_P = 4I/[h_S(h_E + h_W)]. \qquad (4)$$

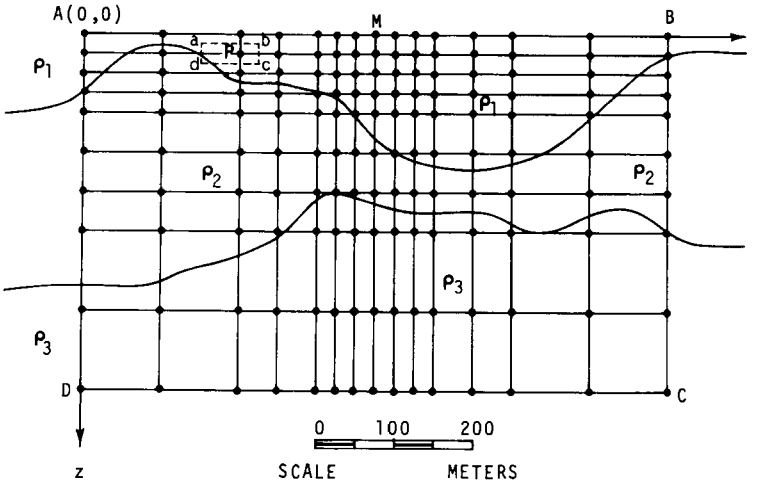

FIG. 1. A discretized model of a geologic structure with resistivities ρ_1, ρ_2, and ρ_3.

Equation (4) represents the strength of the source when the current electrode is located at the surface of the ground.

In the case of uniform intervals between the various elements, we can write

$$h_N = h_S = h_E = h_W = h.$$

For this case

$$q_P = I/h^2. \tag{3a}$$

Also when $h_S = h_E = h_W = h$ and $h_N \neq h$ is allowed to vary such that P approaches the surface, we get

$$\lim_{h_N \to 0} q_P = 2I/h^2. \tag{4a}$$

Equations (3a) and (4a) show that the effective strength of the source is doubled when a given amount of current is supplied at the surface of the ground instead of inside the medium—a fact which is well known from the analytical analysis of the resistivity problem (Van Nostrand and Cook, 1966, p. 42).

Let G denote the set of elements located inside the boundary $ABCDA$ (Figure 1) and Γ the set located on the boundary $ABCDA$. If Γ_1 denotes the set of elements corresponding to the surface boundary AB and Γ_2 the elements along the subsurface boundary $BCDA$, we can write

$$\Gamma = \Gamma_1 \cup \Gamma_2. \tag{5}$$

In terms of finite-difference modeling, we want to evaluate the potential function $v_{i,j}$ for a set of elements $(i, j) \in G \cup \Gamma_1$, subject to the following boundary conditions:

(a) $v_{i,j} = f(x, z)$ along Γ_2, where the function $f(x, z)$ is either given or can be computed by other means for the set of elements $(i, j) \in \Gamma_2$.

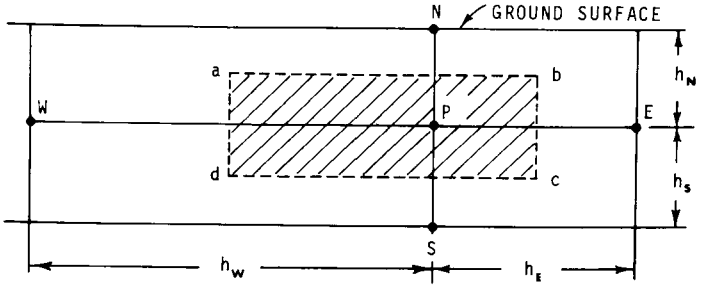

FIG. 2. An element P representing a current source in the discrete model.

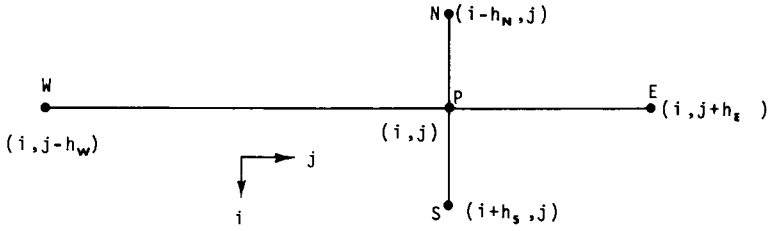

FIG. 3. An arbitrarily chosen element P of the discrete model with its four immediate neighbors, E, N, W, and S.

(b) $\partial v/\partial z = 0$ for the elements $(i, j) \in \Gamma_1$.

(c) $q_{i,j} = 0$, except for a subset $W \in G \cup \Gamma_1$.

In resistivity surveying, $q_{i,j} \neq 0$ only at two elements along Γ_1, each corresponding to the location of a current electrode.

DERIVATION OF FINITE-DIFFERENCE EQUATIONS

Let us consider an arbitrarily chosen element $P(i, j) \in G$ along with its four immediate neighbors, E, N, W, and S (Figure 3). By making use of (2), we shall derive a difference-approximation for the potential $v_{i,j}$ at P in terms of the potentials at its neighboring elements.

On account of the central-difference formula (Smith, 1965, p. 6), the following approximate relation is valid at the point P.

$$\left(\frac{\partial v}{\partial x}\right)_{i,j} = \frac{v_{i,j+h_E/2} - v_{i,j-h_W/2}}{(h_E + h_W)/2}. \quad (6)$$

Therefore, for the point $(i, j + h_E/2)$ we can write

$$\left(\frac{\partial v}{\partial x}\right)_{i,j+h_E/2} = h_E^{-1}(v_{i,j+h_E} - v_{i,j}), \quad (7)$$

$$\left(\sigma \frac{\partial v}{\partial x}\right)_{i,j+h_E/2} = \sigma_{i,j+h_E/2} h_E^{-1}(v_{i,j+h_E} - v_{i,j}). \quad (8)$$

Similarly, for the point $(i, j - h_W/2)$ we get

$$\left(\sigma \frac{\partial v}{\partial x}\right)_{i,j-h_W/2} = \sigma_{i,j-h_W/2} h_W^{-1}(v_{i,j} - v_{i,j-h_W}). \quad (9)$$

A second application of the central-difference formula yields

$$\left[\frac{\partial}{\partial x}\left(\sigma \frac{\partial v}{\partial x}\right)\right]_{i,j} = \frac{2}{h_E + h_W}\left[\left(\sigma \frac{\partial v}{\partial x}\right)_{i,j+h_E/2} - \left(\sigma \frac{\partial v}{\partial x}\right)_{i,j-h_W/2}\right] = \frac{2}{h_E + h_W}\left[\frac{\sigma_{i,j+h_E/2}}{h_E}(v_{i,j+h_E} - v_{i,j}) - \frac{\sigma_{i,j-h_W/2}}{h_W}(v_{i,j} - v_{i,j-h_W})\right]. \quad (10)$$

Continuing in this fashion, one can obtain the self-adjoint finite-difference equivalent of (2) in the following form:

$$\frac{2}{h_E + h_W}\left[\frac{\sigma_{i,j+h_E/2}}{h_E}(v_{i,j+h_E} - v_{i,j}) - \frac{\sigma_{i-h_N/2,j}}{h_N}(v_{i,j} - v_{i-h_N,j})\right] + \frac{2}{h_N + h_S}\left[\frac{\sigma_{i+h_S/2,j}}{h_S}(v_{i+h_S,j} - v_{i,j}) - \frac{\sigma_{i-h_N/2,j}}{h_N}(v_{i,j} - v_{i-h_N,j})\right] + q_{i,j} = 0, \quad (11)$$

where $q_{i,j}$ is given by (3). We can rewrite (11) in an abbreviated form:

$$\alpha_E v_{i,j+h_E} + \alpha_N v_{i-h_N,j} + \alpha_W v_{i,j-h_W} + \alpha_S v_{i+h_S,j} - \alpha_P v_{i,j} + q_{i,j} = 0, \quad (12)$$

where

$$\left.\begin{aligned}\alpha_E &= 2\sigma_{i,j+h_E/2}[h_E(h_E + h_W)]^{-1}\\ \alpha_N &= 2\sigma_{i-h_N/2,j}[h_N(h_N + h_S)]^{-1}\\ \alpha_W &= 2\sigma_{i,j-h_W/2}[h_W(h_E + h_W)]^{-1}\\ \alpha_S &= 2\sigma_{i+h_S/2,j}[h_S(h_N + h_S)]^{-1}\\ \alpha_P &= \alpha_E + \alpha_N + \alpha_W + \alpha_S.\end{aligned}\right\} \quad (13)$$

Hitherto we have assumed that $P(i, j) \in G$. Now let $P(i, j) \in \Gamma_1$, i.e., it is located on the surface of the ground (Figure 4). Since $z = 0$ corresponds to the first row of elements, the coordinates of the element P will be $(1, j)$. Let us temporarily introduce a fictitious row of elements above the surface of the ground such that

$$\left.\begin{aligned}h_N &= h_S;\\ \sigma_{1-h_N,j} &= \sigma_{1+h_S,j},\\ j &= 1, 2, \cdots, n.\end{aligned}\right\} \quad (14)$$

Consequently,

$$\alpha_N = \alpha_S. \quad (15)$$

For the elements $(1, j)$ we must have

$$\left.\frac{\partial v}{\partial z}\right|_{z=0} = 0.$$

This condition will be satisfied if we set

$$v_{1+h_S,j} = v_{1-h_N,j}. \quad (16)$$

In view of (15) and (16), (12) can now be replaced by

$$\alpha_E v_{1,j+h_E} + 2\alpha_S v_{1+h_S,j} + \alpha_W v_{1,j-h_W} - \alpha_P v_{1,j} + q_{1,j} = 0, \quad (17)$$

where $q_{1,j}$ is given by (4).

Let us now consider the case of uniform intervals by setting

$$h_E = h_W = h_N = h_W = h. \quad (18)$$

By a suitable choice of scale we can set $h = 1$. Relation (12) now simplifies to

$$\alpha_E v_{i,j+1} + \alpha_N v_{i-1,j} + \alpha_W v_{i,j-1} + \alpha_S v_{i+1,j} - \alpha_P v_{i,j} + q_{i,j} = 0, \quad (19)$$

and

$$\left.\begin{aligned}\alpha_E &= \sigma_{i,j+1/2} = (\sigma_{i,j} + \sigma_{i,j+1})/2\\ \alpha_N &= \sigma_{i-1/2,j} = (\sigma_{i,j} + \sigma_{i-1,j})/2\\ \alpha_W &= \sigma_{i,j-1/2} = (\sigma_{i,j} + \sigma_{i,j-1})/2\\ \alpha_S &= \sigma_{i+1/2,j} = (\sigma_{i,j} + \sigma_{i+1,j})/2\\ \alpha_P &= 2\sigma_{i,j} + (\sigma_{i,j+1} + \sigma_{i-1,j} + \sigma_{i,j-1} + \sigma_{i+1,j})/2.\end{aligned}\right\} \quad (20)$$

When the element $P(i, j)$ is located in the surface of the ground (19) reduces to

$$\alpha_E v_{1,j+1} + 2\alpha_S v_{2,j} + \alpha_W v_{1,j-1} - \alpha_P v_{1,j} + q_{1,j} = 0. \quad (21)$$

It may be recalled that when $P(1, j)$ corresponds to the negative current electrode, $q_{1,j}$ must be replaced by $-q_{1,j}$; when it corresponds to a potential electrode, $q_{1,j} = 0$.

We are now in a position to evaluate $v_{i,j}$ at all elements $(i,j) \in G \cup \Gamma_1$ in terms of the potential at their four immediate neighbors. Since $v_{i,j}$ for $(i, j) \in \Gamma_2$ will be supplied, we have taken care of the entire set of elements $(i, j) \in G \cup \Gamma$.

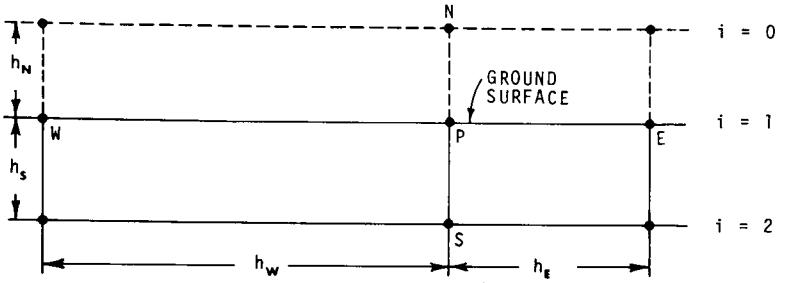

FIG. 4. Neumann type boundary containing a current source P.

EVALUATION OF THE POTENTIAL FIELD

Resistivity matrix

Let the area $ABCD$ (Figure 1) be replaced by a set of $(m + 1)(n + 2)$ elements as illustrated in Figure 5. The problem is to compute the values of the potential $v_{i,j}$ for $(i,j) \in G \cup \Gamma_1$, $(i = 1, 2, \cdots, m; j = 1, 2, \cdots n)$, when the set of values $v(i,j)$ for $(i,j) \in \Gamma_2$ is given. For solving practical problems, both m and n must be quite large. However, for the purpose of understanding some of the details to follow it would suffice to consider a very small field obtained by setting $m = n = 3$ (Figure 6). In order to simplify the treatment we shall assume uniform grid intervals, although this treatment is equally valid for nonuniform grid intervals. We shall express the potential at each point in terms of the potential at its four immediate neighbors and the set of coefficients α_E, α_N, α_W, α_S, and α_P introduced previously. But since we are now dealing with more than one element, each associated with its own four neighbors, it is convenient to express the set of coefficients as $\alpha_E(k)$, etc., where (k) indicates the location of the element under consideration. In Figure 6, $v_{10}, v_{11}, \cdots, v_{18}$ are given, and we want to compute $v_1, v_2, \cdots, v_9$ with the help of (19) and (21).

For element 1, (21) leads to the equation

$$-\alpha_P(1)v_1 + \alpha_E(1)v_2 + 2\alpha_S(1)v_4 + \alpha_W(1)v_{10} + q_P(1) = 0. \quad (22)$$

By placing the known terms on the right-hand side, (22) can be expressed as

$$\alpha_P(1)v_1 - \alpha_E(1)v_2 - 2\alpha_S(1)v_4 = q_P(1) + \alpha_W(1)v_{10} = b_1. \quad (23)$$

Similarly, for the remaining eight elements we have

$$\alpha_P(2)v_2 - \alpha_E(2)v_3 - \alpha_W(2)v_1 - 2\alpha_S(2)v_5 = q_P(2) = b_2, \quad (24)$$

$$\alpha_P(3)v_3 - \alpha_W(3)v_2 - 2\alpha_S(3)v_6 = q_P(3) + \alpha_E(3)v_{18} = b_3, \quad (25)$$

$$\alpha_P(4)v_4 - \alpha_E(4)v_5 - \alpha_N(4)v_1 - \alpha_S(4)v_7 = q_P(4) + \alpha_W(4)v_{11} = b_4, \quad (26)$$

$$\alpha_P(5)v_5 - \alpha_E(5)v_6 - \alpha_N(5)v_2 - \alpha_W(5)v_4 - \alpha_S(5)v_8 = q_P(5) = b_5, \quad (27)$$

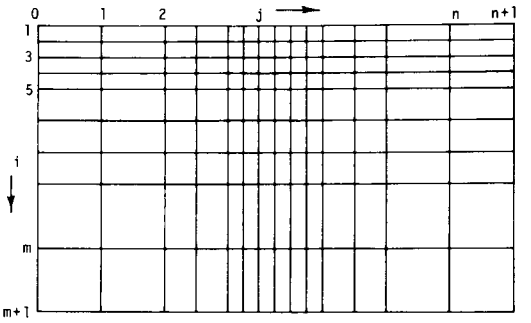

FIG. 5. The area $ABCD$ of Figure 1, discretized into a set of $(m + 1) \times (n + 2)$ elements.

$$\alpha_P(6)v_6 - \alpha_N(6)v_3 - \alpha_W(6)v_5 - \alpha_S(6)v_9 = q_P(6) + \alpha_E(6)v_{17} = b_6, \quad (28)$$

$$\alpha_P(7)v_7 - \alpha_E(7)v_8 - \alpha_N(7)v_4 = q_P(7) + \alpha_W(7)v_{12} + \alpha_S(7)v_{13} = b_7, \quad (29)$$

$$\alpha_P(8)v_8 - \alpha_E(8)v_9 - \alpha_N(8)v_5 - \alpha_W(8)v_7 = q_P(8) + \alpha_S(8)v_{14} = b_8, \quad (30)$$

$$\alpha_P(9)v_9 - \alpha_N(9)v_6 - \alpha_W(9)v_8 = q_P(9) + \alpha_E(9)v_{16} + \alpha_S(9)v_{15} = b_9. \quad (31)$$

In matrix form the system of equations (24) through (31) can be expressed as

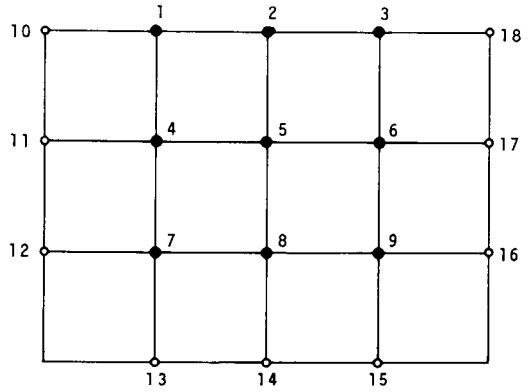

FIG. 6. A simple example of a resistivity model.

$$
\begin{bmatrix}
\alpha_P(1) & -\alpha_E(1) & 0 & -2\alpha_S(1) & 0 & 0 & 0 & 0 & 0 \\
-\alpha_W(2) & \alpha_P(2) & -\alpha_E(2) & 0 & -2\alpha_S(2) & 0 & 0 & 0 & 0 \\
0 & -\alpha_W(3) & \alpha_P(3) & 0 & 0 & -2\alpha_S(3) & 0 & 0 & 0 \\
-\alpha_N(4) & 0 & 0 & \alpha_P(4) & -\alpha_E(4) & 0 & -\alpha_S(4) & 0 & 0 \\
0 & -\alpha_N(5) & 0 & -\alpha_W(5) & \alpha_P(5) & -\alpha_E(5) & 0 & -\alpha_S(5) & 0 \\
0 & 0 & -\alpha_N(6) & 0 & -\alpha_W(6) & \alpha_P(6) & 0 & 0 & -\alpha_S(6) \\
0 & 0 & 0 & -\alpha_N(7) & 0 & 0 & \alpha_P(7) & -\alpha_E(7) & 0 \\
0 & 0 & 0 & 0 & -\alpha_N(8) & 0 & -\alpha_W(8) & \alpha_P(8) & -\alpha_E(8) \\
0 & 0 & 0 & 0 & 0 & -\alpha_N(9) & 0 & -\alpha_W(9) & \alpha_P(9)
\end{bmatrix}
\begin{bmatrix} v_1 \\ v_2 \\ v_3 \\ v_4 \\ v_5 \\ v_6 \\ v_7 \\ v_8 \\ v_9 \end{bmatrix}
=
\begin{bmatrix} b_1 \\ b_2 \\ b_3 \\ b_4 \\ b_5 \\ b_6 \\ b_7 \\ b_8 \\ b_9 \end{bmatrix}. \tag{32}
$$

Relation (32) can be written in abbreviated form

$$\mathbf{Rv} = \mathbf{b}.$$

Here

$$\mathbf{R} = [r_{i,j}],\ i, j = 1, 2, \cdots 9;$$

$$\mathbf{v} = [v_1, v_2, \cdots, v_9];$$

$$\mathbf{b} = [b_1, b_2, \cdots, b_9].$$

Since the elements $r_{i,j}$ of the matrix **R** are directly related to the distribution of resistivities in the subsurface, **R** will be called the resistivity matrix. After several simultaneous permutations of its rows and the corresponding columns, this matrix can be transformed into a tridiagonal block form. A matrix which can be reduced to this form is said to possess property A first formulated by Young (1954). An interesting account of this property of matrices is given by Smith (1965, p. 82).

Another characteristic of matrix **R** which is of interest to us is its directed graph. One can easily verify that the directed graph of this matrix is strongly connected. Those readers who are interested in further details of directed graphs are referred to König (1950).

Stability conditions

Although the above treatment involved a small field ($m = n = 3$), it is obviously applicable to large fields as well. Let us now assume that both m and n are quite large (Figure 5). The number of elements for which we want to compute the field $v_{i,j}$ is mn. Therefore, the resistivity matrix will have the dimensions $N \times N$, where $N = mn$. The system of equations to be solved can be expressed as

$$\sum_{j=1}^{N} r_{i,j} v_{i,j} = b_i, \qquad i = 1, 2, \cdots, N, \tag{33}$$

where $r_{i,j}$ are the elements of **R**. This system can be solved by a successive overrelaxation scheme provided the following conditions are satisfied (Young, 1962):

$$r_{i,i} > 0, \qquad i = 1, 2, \cdots, N. \tag{34a}$$

$$r_{i,i} \geq \sum_{\substack{j=1 \\ j \neq i}}^{N} |r_{i,j}|, \quad i = 1, 2, \cdots, N. \tag{34b}$$

R possesses property A. (34c)

R is irreducible. (34d)

The strict inequality in (34b) must hold for at least one value of i.

An examination of (32), based on the definition of the various coefficients given in (20), will at once reveal that **R** will always satisfy conditions (34a) and (34b), whatever the distribution of resistivities in the subsurface. This, of course, implies that the value of resistivity for each element of the model must lie within a physically meaningful range, viz., $0 < \rho_{i,j} < \infty$ for all $(i,j) \in G \cup \Gamma$. We cannot set $\rho_{i,j} = 0$ or $\rho_{i,j} = \infty$ as is commonly done for simplifying the analytical treatment of the resistivity problem. This is not a real restriction because the geologic materials are neither infinitely conductive nor infinitely resistive. We also note that the requirement of strict inequality included in (34b) is met whenever one of the four immediate neighbors of a point $(i,j) \in G$ is located on the subsurface boundary of the model. It has already been pointed out that **R** fulfills condition (34c). Moreover, a matrix whose directed graph is strongly connected is always irreducible (Varga, 1962, p. 20); consequently, **R** also fulfills condition (34d). It may also be mentioned that **R** will always satisfy condition (34d) as long as it represents a subsurface model which does not consist of two or more physically disconnected zones. If that happens, the current cannot flow between the various zones, and we shall be dealing with more than one independent resistivity problem.

Iterative solution of the potential field

It has already been pointed out that for solving practical problems, the system of equations (33) must be quite large. The potential field can be computed easily by the straightforward method of relaxation due to Southwell (1946). However, this method is much too slow, even on modern high-speed computers. A part of the reason is that the method is not compatible with automatic computations which must proceed according to a prescribed order without human intervention. We shall evaluate the field by the method of successive overrelaxation (SOR) and its very powerful extension known as successive line overrelaxation (SLOR) (Varga, 1962, p. 199).

Let us make an initial guess of the strength of the field $v_{i,j}$, $(i,j) \in G$. Next we improve upon the guess of $v_{i,j}$ by using (19) and (21) in the order of increasing number of rows and in each row in the order of increasing number of columns. That is, we advance across the field from top to bottom and along each row from left to right. The operation of modifying the estimates of $v_{i,j}$ over the entire field will complete one iteration. Let the results obtained at the end of the kth iteration be denoted by $v_{i,j}{}^{k}$. We want to evaluate the vector $\mathbf{v}$ given by

$$\mathbf{v} = \lim_{k \to \infty} \mathbf{v}^{(k)}. \tag{35}$$

In practice the iterative process is switched off when $d^{k} < \epsilon$, where

$$d^{(k)} = \max_{(i,j) \in G \cup \Gamma_1} |v_{i,j}^{(k)} - v_{i,j}^{(k-1)}| \tag{36}$$

and ϵ is a positive quantity whose magnitude depends on the accuracy desired.

Let us imagine that the $(k+1)$th iteration is in progress. With the help of (19) we can write down the following expression for computing $v_{i,j}{}^{k+1}$:

$$\begin{aligned} v_{i,j}^{(k+1)} = [&\alpha_E(i,j)v_{i,j+1}^{(k)} + \alpha_N(i,j)v_{i-1,j}^{(k+1)} \\ &+ \alpha_W(i,j)v_{i,j-1}^{(k+1)} \\ &+ \alpha_S(i,j)v_{i+1,j}^{(k)} + q_{i,j}]/\alpha_P(i,j), \\ i = 2, 3, \cdots, m. \end{aligned} \tag{37}$$

A similar expression for $i = 1$ can be obtained from (21). In (37) we have used the latest values available for computing $v_{i,j}{}^{k+1}$. Thus, the elements located "north" and "west" of the element (i,j) have already been traversed during the $(k+1)$th iteration; therefore, we have used the values $v_{i-1,j}^{k+1}$ and $v_{i,j-1}^{k+1}$ instead of $v_{i-1,j}^{k}$ and $v_{i,j-1}^{k}$. Equation (37) is usually called the Gauss-Seidel relation. The spectral radius of the Gauss-Seidel iteration matrix, which will be needed later on, is defined as

$$\rho(G) = \lim_{m \to \infty} \frac{||\mathbf{v}^{(m)}||}{||\mathbf{v}^{(m-1)}||}, \tag{38}$$

where $||\mathbf{v}^{k}||$ represents the norm of $\mathbf{v}^{k}$ and is given by

$$||\mathbf{v}^{(k)}|| = \sum_{i=1}^{N} \sum_{j=1}^{N} |v_{i,j}^{(k)}|. \tag{39}$$

Relation (37) can be expressed as

$$v_{i,j}^{(k+1)} = v_{i,j}^{(k)} + \frac{\omega}{\alpha_P(i,j)} [\alpha_E(i,j)v_{i,j+1}^{(k)}$$

$$+ \alpha_N(i, j)v_{i-1,j}^{(k+1)} + \alpha_W(i, j)v_{i,j-1}^{(k+1)} + \alpha_S(i, j)v_{i+1,j}^{(k)} + q_{i,j} - \alpha_P(i, j)v_{i,j}^{(k)}], \quad (40)$$

where $\omega = 1$. In SOR, we overrelax the field at every point by using an acceleration parameter $1 < \omega < 2$. When dealing with nonuniform media there is no easy way to determine an optimum value of this parameter. It is commonly determined by using the relation

$$\omega = \frac{2}{1 + [1 - \rho(G)]^{1/2}}, \quad (41)$$

where $\rho(G)$ is given by (38).

In practice, one starts the finite-difference computations by assuming $\omega = 1$ and evaluates $\rho(G)$ periodically, say, at the end of every 5th iteration. After a number of iterations, the variation in the magnitude of $\rho(G)$ becomes less and less and $\rho(G)$ tends to an asymptotic value. This value of $\rho(G)$ is used for computing the optimum value of ω. Experience with resistivity modeling indicates that the optimum value of ω is much more dependent on the order of the resistivity matrix $\mathbf{R}$, and is not very sensitive to changes in magnitude of the elements of $\mathbf{R}$. This is very fortunate because, as long as we do not change the size of the potential field to be investigated, the same value of ω may be used for investigating different models for which the geology does not change drastically.

We shall now describe a more efficient procedure based on the SLOR method for computing the potential field. In the above treatment the set of data $\{v_{i,j}\}$ appeared as an N-dimensional vector. Thus, for the simple model represented by Figure 6, both i and j ranged from 1 to 3 and N was equal to 9. Let us now consider a series of vectors:

$$\mathbf{v}_i = [v_{i,1}, v_{i,2}, \cdots, v_{i,n}], \quad i = 1, 2, \cdots, m. \quad (42)$$

Here m and n denote, respectively, the number of rows and columns defining the elements of the resistivity model. They should not be confused with the rows and columns of the resistivity matrix $\mathbf{R}$, which is a square matrix of order $N = mn$. The components of $\mathbf{v}_i$ given on the right-hand side of (42) represent the values of the potential along the ith row of the model.

The SLOR method is based on computing the improved estimate of $v_{i,j}$ simultaneously along the entire row rather than for each individual element of the model separately. Imagine that the $(k + 1)$th iteration is in progress and we are about to start with the ith row. For the first element along this row ($j = 1$), we can write

$$-\alpha_W(i, 1)v_{i,0} + \alpha_P(i, 1)\tilde{v}_{i,1} - \alpha_E(i, 1)\tilde{v}_{i,2} - \alpha_N(i, 1)v_{i-1,1}^{(k+1)} - \alpha_S(i, 1)v_{i+1,1}^{(k)} - q_{i,1} = 0. \quad (43)$$

In (43), $\tilde{v}_{i,j}$ denotes the elements of an auxiliary vector

$$\tilde{\mathbf{v}}_i = [\tilde{v}_{i,1}, \tilde{v}_{i,2}, \cdots, \tilde{v}_{i,n}], \quad i = 1, 2, \cdots, m,$$

from which we shall compute an improved estimate of the vector $\mathbf{v}_i$ defined by (42).

We also note that $v_{i,0}$ belongs to the boundary and is known; $v_{i+1,1}^{(k)}$ and $v_{i-1,1}^{(k+1)}$ have already been computed, during the kth and $(k + 1)$th iteration, respectively, and can be treated as "known" information. By transferring all the known terms on the right-hand side, (43) can be expressed as

$$\alpha_P(i, 1)\tilde{v}_{i,1} - \alpha_E(i, 1)\tilde{v}_{i,2} = \alpha_N(i, 1)v_{i-1,1}^{(k+1)} + \alpha_S(i, 1)v_{i+1,1}^{(k)} + \alpha_W(i, 1)v_{i,0} + q_{i,1} = t_1. \quad (44)$$

Similarly, for the next $(n - 2)$ elements of the ith row of the model, we can write

$$-\alpha_W(i, j)\tilde{v}_{i,j-1} + \alpha_P(i, j)\tilde{v}_{i,j} - \alpha_E(i, j)\tilde{v}_{i,j+1} = \alpha_N(i, j)v_{i-1,j}^{(k+1)} + \alpha_S(i, j)v_{i+1,j}^{(k)} + q_{i,j} = t_j, \quad j = 2, 3, \cdots, (n - 1). \quad (45)$$

When $j = n$, we have

$$-\alpha_W(i, n)\tilde{v}_{i,n-1} + \alpha_P(i, n)\tilde{v}_{i,n} = \alpha_E(i, n)v_{i,n+1} + \alpha_N(i, n)v_{i-1,n}^{(k+1)} + \alpha_S(i, n)v_{i+1,n}^{(k)} + q_{i,n} = t_n. \quad (46)$$

The system of equations (44), (45), and (46) can be expressed as

$$
\begin{bmatrix}
\alpha_P(i,1) & -\alpha_E(i,1) & & & & & & & \\
-\alpha_W(i,2) & \alpha_P(i,2) & -\alpha_E(i,2) & & & & & & \\
 & -\alpha_W(i,3) & \alpha_P(i,3) & -\alpha_E(i,3) & & & & & \\
 & & \cdots & \cdots & \cdots & & & & \\
 & & & -\alpha_W(i,n-1) & \alpha_P(i,n-1) & -\alpha_E(i,n-1) & & & \\
 & & & & -\alpha_W(i,n) & \alpha_P(i,n) &
\end{bmatrix}
\begin{bmatrix}
\tilde{v}_{i,1} \\ \tilde{v}_{i,2} \\ \cdot \\ \cdot \\ \cdot \\ \tilde{v}_{i,n}
\end{bmatrix}
=
\begin{bmatrix}
t_1 \\ t_2 \\ \cdot \\ \cdot \\ \cdot \\ t_n
\end{bmatrix}. \qquad (47)
$$

In compact notation, (47) is equivalent to

$$\mathbf{R}_i \tilde{\mathbf{v}}_i = \mathbf{t}_i, \qquad i = 1, 2, \cdots, m. \qquad (48)$$

Since $\mathbf{R}_i$ is a tridiagonal matrix, the vector $\tilde{\mathbf{v}}_i$ can be readily determined by the method of Gaussian elimination (Faddeeva, 1959, p. 65). The set of values obtained in this manner is further modified by overrelaxation to obtain the $(k+1)$th estimate of the vector $\mathbf{v}_i$:

$$\mathbf{v}_i^{(k+1)} = \mathbf{v}_i^{(k)} + \omega_l(\tilde{\mathbf{v}}_i - \mathbf{v}_i^{(k)}), \qquad i = 1, 2, \cdots m, \qquad (49)$$

where ω_l represents an optimum value of the acceleration parameter when we are using the SLOR method. The subscript l is used to emphasize the fact that ω_l is different from the parameter ω previously introduced in the discussion of the SOR method; ω_l is given by a relation similar to (41):

$$\omega_l = \frac{2}{1 + [1 - \rho_l(G)]^{1/2}}.$$

$\rho_l(G)$ is the spectral radius of the Gauss-Seidel iteration matrix. In the case of the SLOR method, $\rho_l(G)$ is determined by setting $\omega_l = 1$. Apart from that, the procedure for evaluating $\rho_l(G)$ is exactly the same as the procedure previously described for $\rho(G)$.

CONSIDERATIONS RELATED TO MODEL DESIGN

Problems related to boundaries and grid intervals

When the area $ABCD$ shown in Figure 1 is large and the boundary $BCDA$ is sufficiently far from the current electrodes, we can neglect the amount of current flowing across this boundary. This leads to the following Neumann boundary condition.

$$\left.\begin{aligned} \left.\frac{\partial v(x,z)}{\partial x}\right|_{(i,j)} &= 0, \quad i = 1, 2, \cdots, m+1; \quad j = 0, n+1; \\ \left.\frac{\partial v(x,z)}{\partial z}\right|_{(i,j)} &= 0, \quad j = 0, 1, \cdots, n+1; \quad i = m+1. \end{aligned}\right\} \tag{50}$$

When we are investigating less resistive media, the values of the potential along the boundary $BCDA$ may not be too different from zero; in that case, we can introduce a somewhat simpler Dirichlet boundary condition:

$$v(i,j) = 0, \quad \text{for all} \quad (i,j) \in \Gamma_2. \tag{51}$$

Numerical experiments on resistivity modeling indicate that the size of the resistivity matrix must be extremely large before we can get accurate results by using either (50) or (51); otherwise, (50) leads to an overestimation and (51) an underestimation of the actual field which is only bounded at the surface of the ground. This problem can be overcome by replacing the subsurface boundary by a strip of material of large effective width, as shown in Figure 7(a). Imagine that we set up a model by using uniform grid intervals everywhere, including the zone occupied by the termination strip. Within the strip, the resistivities $\rho_1, \rho_2, \cdots$ are assigned as if it were a natural extension of the structures under investigation. After that, the strip is expanded outward without modifying the resistivities. An enlarged view of a portion of the expanded strip is shown in Figure 7(b). We observe that the grid intervals in the zone of interest are still uniform, but within the strip they are expanded horizontally in three large steps. As a result, the structures enclosed by $ABCDA$ now become a "local" perturbation in a much larger zone enclosed by the external boundary of the model $A'B'C'D'A'$. This zone would be sufficiently large provided we get virtually identical results in the inner zone $ABCDA$, irrespective of whether we use (50) or (51) along the boundary $B'C'D'A'$ for evaluating the potential field.

Optimization studies along these lines suggest that the effects of the subsurface boundaries become negligible when we set the intervals BE, EF, and FB' equal, respectively, to 10, 100, and 1000 times the grid intervals used for discretizing the area $ABCD$. The same argument applies to the horizontal portion of the termination strip, except that the grid intervals are expanded downward. For most problems, accurate results can be obtained by dividing the horizontal distance AB into 50 intervals and the vertical distance BC into 25 intervals. It may be pointed out that a modeling system based on the self-adjoint equation remains stable for all values of grid intervals. Consequently, the actual values of the grid intervals may be assigned arbitrarily, depending upon the accuracy with which the model is expected to represent the subsurface geology.

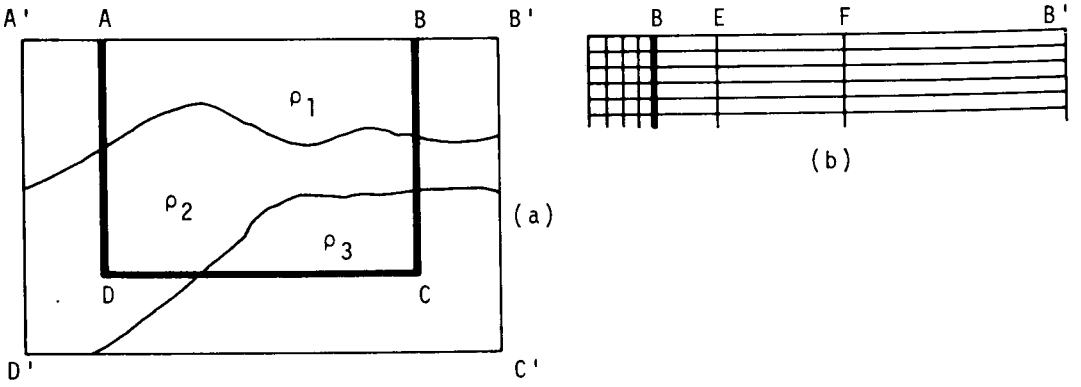

FIG. 7. (a) Extension of a resistivity model of an arbitrary structure by a termination strip. (b) An enlarged view of a portion of this strip.

Manipulation of coefficients

The efficiency of the finite-difference evaluation of the potential field is heavily dependent upon those calculations which occur repeatedly. Thus, in the SOR evaluation of the field, the use of (40) will form the bulk of the computations. Therefore, the set of coefficients α_E, α_W, α_N, α_S, and α_P for each (i, j) must be computed only once before the iterations begin. Further examination of (40) will suggest that this relation should preferably be used in the form

$$v_{i,j}^{(k+1)} = (1 - \omega)v_{i,j}^{(k)} + \omega[\beta_E(i, j)v_{i,j+1}^{(k)} + \beta_N(i, j)v_{i-1,j}^{(k+1)} + \beta_W(i, j)v_{i,j-1}^{(k+1)} + \beta_S(i, j)v_{i+1,j}^{(k)} + \gamma_{i,j}], \quad (52)$$

where

$$\gamma_{i,j} = q_{i,j}/\alpha_P(i, j),$$

$$\beta_E(i, j) = \alpha_E(i, j)/\alpha_P(i, j), \text{ etc.}$$

A comparison of (40) and (52) suggests that repeated divisions by $\alpha_P(i, j)$ as implied by (40) can be avoided by computing the coefficients $\beta_{E(i,j)}$, etc., in advance. Moreover, instead of storing the five coefficients α_E, α_W, α_N, α_S, and α_P for each (i, j), we now need only the four coefficients β_E, β_W, β_N, and β_S for each (i, j), thereby reducing the size of the computer memory required for storing the coefficients.

APPLICATIONS

Several computer programs based on the treatment presented above were developed and used for computing the potential field and apparent resistivity curves for various structures. Some of the structures selected for this purpose possessed a simple geometry, and their field could also be computed analytically. This afforded a comparison of analytical results with the data obtained by the use of the corresponding finite-difference models.

Two parallel layers

The potential field inside a parallel-layer earth due to a pair of infinite-line electrodes located at the surface has been investigated by Peters and Bardeen (1930). When there are only two layers and the origin corresponds to the midpoint of the line joining the electrodes, the potential at any point (x, z) in the subsurface is given by

$$v_1(x, z) = \sum_{n=0}^{\infty} \left(\frac{\gamma - 1}{\gamma + 1}\right)^n f(x; 2nh_1 - z) + \sum_{n=1}^{\infty} \left(\frac{\gamma - 1}{\gamma + 1}\right)^n f(x; 2nh_1 + z), \quad (53)$$

$$v_2(x, z) = \frac{2\gamma}{1 + \gamma} \sum_{n=0}^{\infty} \left(\frac{\gamma - 1}{\gamma + 1}\right)^n \cdot f(x; 2nh_1 + z), \quad (54)$$

where

$$f(x; z) \equiv v(x, z) = \frac{I\rho_1}{2\pi} \ln \frac{(x + L/2)^2 + z^2}{(x - L/2)^2 + z^2}. \quad (55)$$

L is the distance between the current electrodes; h_1 is the thickness of the first layer; $\gamma = \rho_2/\rho_1$; and I is the current per unit length of the line electrodes. Relations (53) and (54) give the potential in layers 1 and 2, respectively, whereas (55) represents the potential $v(x, z)$ of a uniform medium with resistivity ρ_1. When $\gamma = 1$, both (53) and (54) are reduced to (55).

We computed the potential field of a structure consisting of two parallel layers analytically by using (53) and (54) and also by means of the finite-difference scheme. The computations were based on the following parameter values:

resistivity of the upper layer, $\rho_1 = 100$ ohm-m;
resistivity of the lower layer, $\rho_2 = 30$ ohm-m;
thickness of the upper layer, $h_1 = 20$ length units;
current electrode separation, $L = 20$ length units;
current, $I = 25$ ma/unit length.

A short reflection on (53) and (54) will indicate that the results do not depend on the specific unit of length used. Thus, in Figure 8, which gives the computed equipotential lines, the unit of length corresponds to 20 m; but if the unit of length were 30 m, the same field would represent a structure whose upper layer is 600 m thick and receives current at the rate of 25 ma/(30 m) from a pair of line electrodes 600 m apart. The field shows a break in the equipotential lines all along the interface between the two layers. These data are in excellent agreement with the analytical results except in the immediate vicinity of the lower boundary of the model.

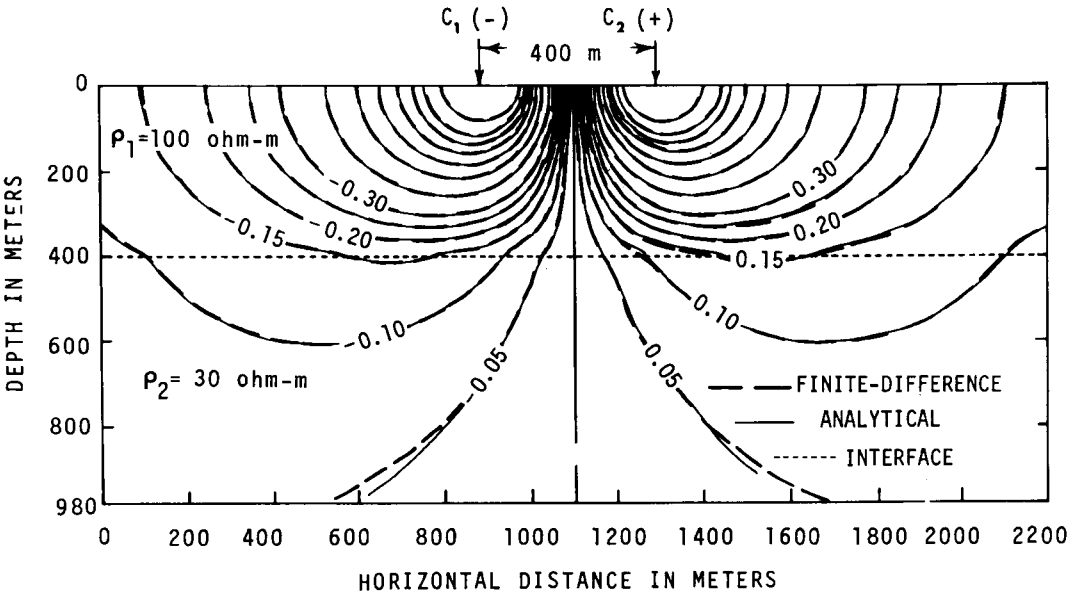

FIG. 8. The potential for a two-layer structure computed by finite-difference modeling (broken lines) and the corresponding analytical results (continuous lines).

Structure containing a dipping interface

The structure investigated is shown in Figure 9. The interface OE separating materials of resistivity ρ_1 and ρ_2 is assumed to be so oriented that the direction of the strike is parallel to the direction of the line electrodes. $ABCDA$ defines the boundary of the finite-difference model. When $\rho_2 \ll \rho_1$ or $\rho_2 \gg \rho_1$, the potential along the surface of the ground can be computed analytically (Peters and Bardeen, 1930). Let r_1 and r_2 denote the distances of the current line-electrodes C_1 and C_2, respectively, from the point 0, taken as the origin of the polar coordinates (r, θ). If the dip angle is $\alpha = \pi/2n$, where n is an integer and $\rho_2 \to 0$, the potential at any point $P(r, 0)$, located at the surface of the ground ($\theta = 0$), is given by

$$v(r) = \frac{I\rho_1}{\pi}\left[\frac{1}{2}\ln\left(\frac{r_1 - r}{r_2 - r}\right)^2 + (-1)^n \ln\frac{r_1 + r}{r_2 + r} + \sum_{k=1}^{n-1}(-1)^k \ln\frac{r_1^2 + r^2 - 2r_1 r\cos(k\pi/n)}{r_2^2 + r^2 - 2r_2 r\cos(k\pi/n)}\right]. \quad (56)$$

In the finite-difference model the values of the potential along the boundary BCE were obtained

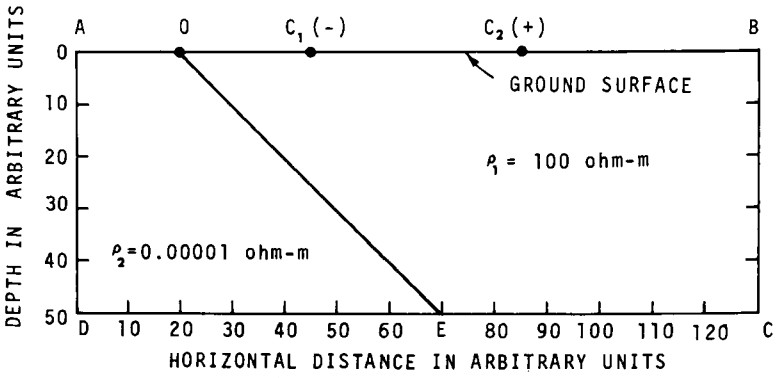

FIG. 9. A structure containing a dipping interface.

with the help of (55) by assuming a uniform medium of resistivity ρ_1; for the rest of the subsurface boundary, viz., EDA, the potential was set equal to zero. The field was computed by assuming the following parameter values:

$r_1 = 26$ length units,
$r_2 = 66$ length units,
$\rho_1 = 100$ ohm-m,
$\rho_2 = 0.00001$ ohm-m,
$\alpha = 45$ degrees,
$I = 25$ ma/unit length.

The results are presented in Figure 10; they are virtually identical with the corresponding results obtained analytically.

Evaluation of apparent resistivity curves by the reciprocity theorem

A computational shortcut which renders finite-difference modeling ideally suited to the evaluation of vertical-sounding apparent resistivity curves for the line-source Schlumberger configuration can be explained as follows. In a finite-difference model, the location of electrodes will correspond to the surface elements $(1, j) \in \Gamma_1$, $j = 1, 2, \cdots, n$. Let L denote the distance between the current line-electrodes C_1 and C_2, and l the distance between the potential electrodes P_1 and P_2. In order to simulate the Schlumberger configuration, in which the point-electrodes are planted symmetrically with respect to the center of the sounding station, it would be convenient to make n an odd integer. Then the location of the electrodes will correspond to the following elements of the model:

$$\left.\begin{aligned} &\text{element } (1, r) \quad \text{for} \quad P_1; \\ &\qquad r = (n + 1)/2 - l/2; \\ &\text{element } (1, s) \quad \text{for} \quad P_2; \\ &\qquad s = (n + 1)/2 + l/2; \end{aligned}\right\} \qquad \left.\begin{aligned} &\text{element } (1, a) \quad \text{for} \quad C_1; \\ &\qquad a = (n + 1)/2 - L/2; \\ &\text{element } (1, b) \quad \text{for} \quad C_2; \\ &\qquad b = (n + 1)/2 + L/2. \end{aligned}\right\} \tag{57}$$

The apparent resistivity of the ground in the case of a line-source dipole (Parasnis, 1965) is given by

$$\rho_a(L) = \frac{\pi}{2}\left(\ln\frac{L + l}{L - l}\right)^{-1}\frac{\Delta v}{I}, \tag{58}$$

where Δv is the potential difference across P_1 and P_2 and I denotes current flowing into the ground per unit length of the line-source dipole. Ideally, $l \ll L$; in that case (58) reduces to

$$\rho_a(L) \cong \frac{\pi}{4}\frac{L}{l}\frac{\Delta v}{I}. \tag{59}$$

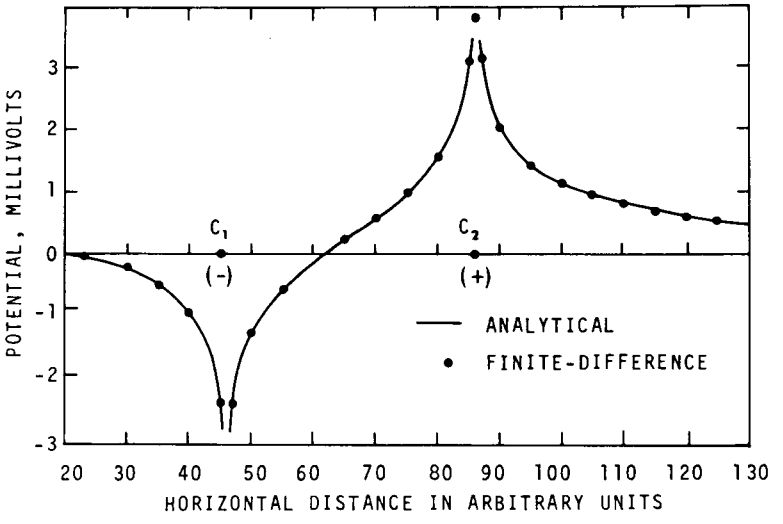

FIG. 10. The distribution of potential along the surface of the structure shown in Figure 9 due to a line-source dipole C_1 and C_2. Results of analytical and finite-difference computations are shown.

In order to keep l as small as possible, let us choose $l = 2$ in the model; then the potential electrodes will correspond to the elements $[1, (n - 1)/2]$ and $[1, (n + 3)/2]$. Since the model allows for the computation of all the values $v_{i,j}$, $j = 1, 2, \cdots, n$, the potential difference across these elements can readily be obtained. An apparent resistivity curve represents a set of observations obtained by keeping the positions of P_1 and P_2 fixed and successively increasing the value of L. Imagine that we compute the potential field again by changing the separation between C_1 and C_2 to L'. C_1 and C_2 will now correspond to the elements $(1, a')$ and $(1, b')$, in accordance with (57), and the apparent resistivity will be given by

$$\rho_a(L') = \frac{\pi}{2}\left(\ln\frac{L' + l}{L' - l}\right)^{-1}\frac{\Delta v'}{I}. \quad (60)$$

In (60), $\Delta v'$ represents the potential difference across the elements $[1, (n - 1)/2]$ and $[1, (n + 3)/2]$ due to the new position of the current electrodes. Note that we have used the same amount of current in the two modeling experiments.

At this stage we shall make use of the reciprocity theorem (Jordan and Balmain, 1968, p. 347), which states that if a current is applied to an isotropic physical system at one pair of terminals and the open-circuit voltage is measured at a second pair of terminals, the ratio of voltage to current remains the same when the positions of the current source and the voltmeter are interchanged. In our case we are dealing with apparent resistivity, which is nothing but a normalized value of this ratio. Consequently, in the first modeling experiment, if we had shifted the current electrodes to the elements $(1, r)$ and $(1, s)$, the potential drop across the elements $(1, a)$ and $(1, b)$ a distance L apart would again be Δv. By the same reasoning, the voltage across $(1, a')$ and $(1, b')$ must be $\Delta v'$, because this setting of electrodes results from interchanging the current and potential electrodes in the second experiment. This observation leads to an important conclusion:

By selecting a model size sufficiently large that it accurately represents the resistivity distribution over the zone of interest, the entire resistivity curve can be computed in a single step. All we need to do is compute the potential field at all those locations which are actually occupied by the current point-electrodes in an expanding Schlumberger configuration and by locating the current line-electrodes at the elements of the model which actually correspond to the original field location of the potential electrodes. When great depths are involved, the size of the resistivity matrix may become too large. This problem can be avoided if we use nonuniform grid intervals, taking care that these intervals get smaller as the current elec-

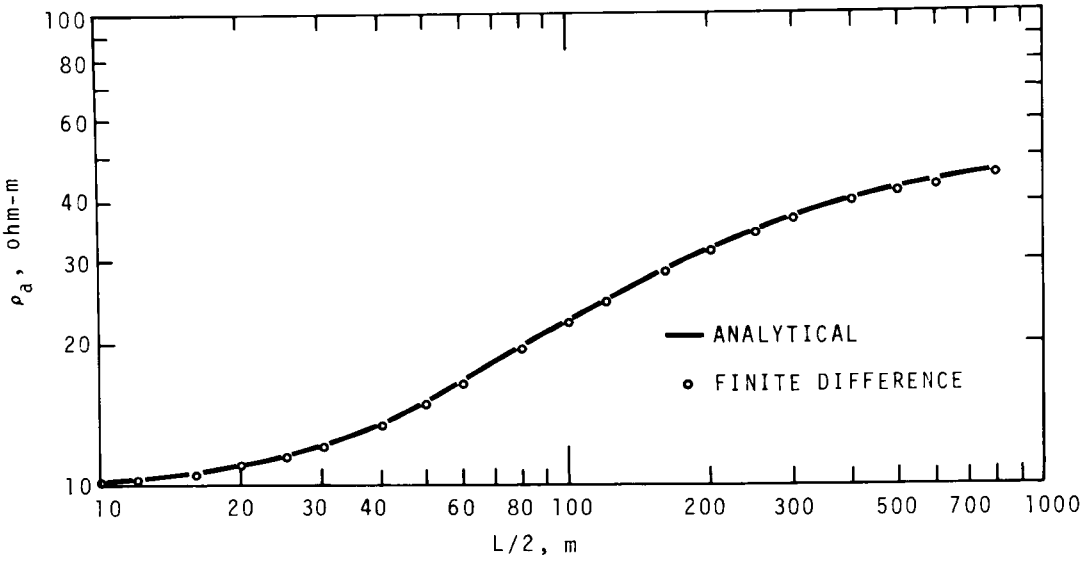

FIG. 11. Computed apparent resistivity curve for a Schlumberger type line-source array vertical sounding of a two-layer structure. Results for analytical and finite-difference calculations are shown.

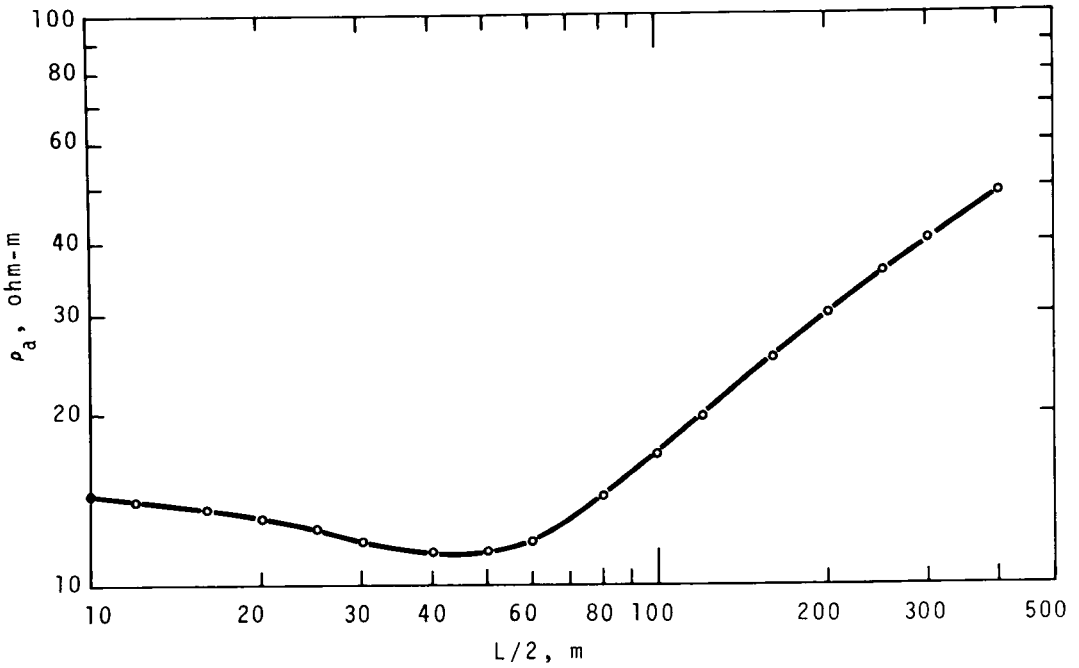

FIG. 12. Computed vertical sounding apparent resistivity curve for the structure shown in Figure 1. A Schlumberger type line-source array was assumed.

trodes are approached. It must also be remembered that the choice of the grid intervals should be such that the various subsurface interfaces of the structure under investigation run, as far as possible, half-way between the neighboring elements of the model. This is an important consideration which will become more obvious from the boundary of the hatched zone shown in Figure 2. Figure 11 shows a computed apparent resistivity profile for a Schlumberger-type line-source array on a structure consisting of two parallel layers. The calculations were carried out by assuming ρ_1 = 10 ohm-m, ρ_2 = 50 ohm-m, and h_1 = 40 m. The continuous curve represents analytically computed data, and the values obtained by finite-difference modeling are indicated by circles.

The cases presented so far demonstrate that, for all practical purposes, the results obtained by finite-difference modeling are as accurate as those obtained by analytical means.

Apparent resistivity curve for a complex structure

Figure 12 shows the computed apparent resistivity curve for the geologic structure shown in Figure 1. The curve corresponds to ρ_1 = 15 ohm-m, ρ_2 = 3 ohm-m, and ρ_3 = 75 ohm-m; it was computed by assuming the Schlumberger-type line-source configuration with its center located at point *M* (Figure 1).

CONCLUDING REMARKS

The resistivity method has been widely used for the exploration of groundwater. Its success in this particular area of exploration is at least partly due to the fact that the assumption of a parallel-layer earth, which forms the basis of conventional procedures of resistivity data interpretation, is usually applicable to the occurrence of groundwater in nature. Since both gas- and oil-bearing formations possess high resistivity, this method should in principle be suitable to exploration for hydrocarbons as well.

The finite-difference modeling system presented by the author was developed for evaluating potential fields and vertical sounding apparent resistivity curves for complex geologic structures commonly associated with the occurrence of hydrocarbons. The entire treatment was restricted to two dimensions and the use of a line-source dipole. Some of the structures investigated possessed a simple geometry, and they could also be treated analytically. In such cases the results ob-

tained by finite-difference modeling were virtually identical to the corresponding values computed analytically. This suggests that finite-difference modeling is a very powerful tool capable of yielding accurate results for a large variety of two-dimensional geologic structures. The procedure outlined above can be extended to accommodate three-dimensional structures and a point-source dipole. Unfortunately, the use of three-dimensional finite-difference models implies prohibitive computer costs. We hope that this apparent drawback will dwindle with the rapidly growing use of minicomputers. In the opinion of the author, however, a more practical approach would be to transform line-source potential fields computed for two-dimensional structures into the corresponding point-source fields along the lines described by Tranter (1956). The computational effort required for such a transformation can be greatly reduced by the use of the fast Fourier transform (Brigham and Morrow, 1967).

ACKNOWLEDGMENTS

The author is indebted to Dr. W. G. Clement, Dr. Rup K. Kaul, and Dr. Sven Treitel for suggestions and criticisms; to Dr. S. N. Domenico and Dr. A. C. Reynolds for reviewing the manuscript; and to Rida Bakbak for sharing a significant burden of programming. Permission from Amoco Production Co. to publish this work is greatly appreciated.

REFERENCES

Aiken, C. L., Hastings, D. A., and Sturgul, J. R., 1973, Physical and computer modeling of induced polarization: Geophys. Prosp., v. 21, p. 763–782.

Brigham, E. O., and Morrow, R. E., 1967, The fast Fourier transform: IEEE Spectrum, v. 4, p. 63–70.

Faddeeva, V. N., 1959, Computational methods of linear algebra: New York, Dover Publications, Inc., Translated from Russian by Curtis D. Benster.

Jepsen, A. F., 1969, Resistivity and induced polarization modeling: Ph.D. dissertation, University of California, Berkeley.

Jordan, E. C., and Balmain, K. G., 1968, Electromagnetic waves and radiating systems: Englewood Cliffs, Prentice-Hall, Inc.

König, D., 1950, Theorie der endlichen und unendlichen Graphen: New York, Chelsea Publishing Co.

Parasnis, D. S., 1965, Theory and practice of electric potential and resistivity prospecting using linear current electrodes: Geoexploration, v. 3, p. 3–69.

Peters, L. J., and Bardeen, J., 1930, The solution of some theoretical problems which arise in electrical methods of geophysical exploration: University of Wisconsin Eng. Expt. St. Bull. 71.

Smith, G. D., 1965, Numerical solution of partial differential equations: New York, Oxford University Press.

Southwell, R. V., 1946, Relaxation methods in theoretical physics, v. 1: London, Oxford University Press.

Tranter, C. J., 1956, Integral transforms in Mathematical physics: New York, John Wiley & Sons, Inc.

Van Nostrand, R. G., and Cook, K. L., 1966, Interpretation of resistivity data: USGS Prof. paper 449, Washington, D.C., U.S. Govt. Printing Office.

Varga, R. S., 1962, Matrix iterative analysis: Englewood Cliffs, Prentice-Hall, Inc.

Young, D., 1962, The numerical solution of elliptic and parabolic partial differential equations, *in* Survey of numerical analysis: New York, McGraw-Hill Book Co., Inc., p. 380-438.

Young, D., 1954, Iterative methods for solving partial difference equations of elliptic type: Trans. Am. Math. Soc., v. 76, p. 92–111.